Planar array of semiconducting nanotubes in external electric field: Collective screening and polarizability

T. A. Sedrakyan, E. G. Mishchenko, and M. E. Raikh

Department of Physics, University of Utah, Salt Lake City, UT 84112
(Dated: February 6, 2008)

We study theoretically the charge separation in a planar array of semiconducting nanotubes (NTs) of length, $2h$, placed in external electric field, F, parallel to their axes. By employing the conformal mapping, we find analytically the *exact* distribution of the induced charge density for arbitrary ratio of the gap, E_g, and the voltage drop, eFh, across the NT. We use the result obtained to (*i*) trace the narrowing of the neutral strip at center of the NT with increasing F; (*ii*) analyze the polarizability of the array as a function of E_g; (*iii*) study the field enhancement near the tips.

PACS numbers: 73.63.Fg, 77.84.Lf, 79.60.Ht

I. INTRODUCTION

During the past decade much progress has been achieved in growth of vertically aligned arrays of carbon nanotubes (NTs). Vertical alignment is attractive for such applications as field emission displays[1,2,3,4,5,6,7] and chemical sensors[8]. Latest publications[9,10,11,12] report almost perfect alignment. Since recently, the efforts of researchers were also directed at synthesis of nantobube arrays aligned *in a plane* [13,14,15,16,17,18]. The objective of this effort is the synthesis of complex organized NT structures for integrated molecular electronics devices and optoelectronic applications. Growth and patterning of in-plane oriented arrays require novel technological approaches. A number of such approaches have been proposed in Refs. 14,15,18, and successfully implemented.

A planar array of NTs is shown schematically in Fig. 1. In a typical experimental situation the distance, d, between the neighboring NTs in the array is much smaller than the length, $2h$, of the constituting NTs. This suggests that the response of the array to the external electric field must exhibit a *collective* character. For vertically oriented arrays, the collective electrostatic response has been previously discussed in the literature[19,20,21]. This response plays a crucial role in designing the NT-based field emitters. For planar arrays, being the emerging area of research, their collective electrostatic properties have never been addressed.

Intuitively, it is obvious that responses of vertical and planar arrays to external electric field are dramatically different. Indeed, external field does not penetrate into a dense enough vertical array much deeper than the intertube distance[20]. In other words, to the first approximation, the tops of NTs constituting the vertical array can be considered as a metallic plate. By contrast, for a planar array, the force lines of external field can extend "above" and "below" the NT plane (see Fig. 1b), thus causing the charge separation within each NT, constituting the array. The collective character of the electrostatic response manifests itself in the fact that the *actual field*, causing this separation in a given NT is strongly
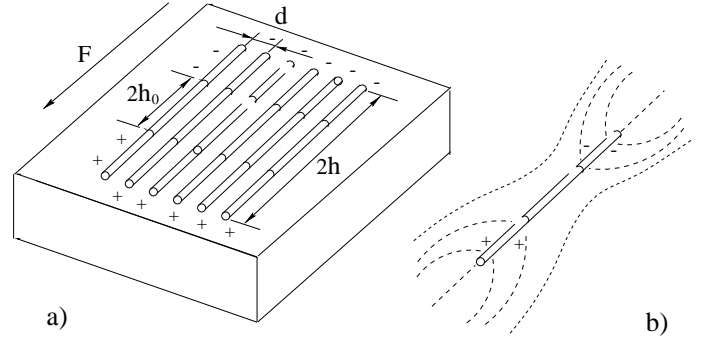

FIG. 1: a) a planar array of semiconducting NTs in external field, F, is shown schematically; d is the distance between the neighboring NTs. As a result of charge separation, the positively and negatively charged regions of length, $h-h_0$, emerge near the tips. These regions are separated by neutral strips of width $2h_0$; b) Force lines of electric field above and below the array are curved as a result of the charge separation. In charged regions the force lines enter (exit) the NTs normally to the plane of the array.

altered by the presence of the neighboring NTs. The resulting dipole moment, induced in an individual NT within the planar array, depends on the charge distribution, the form of which is not obvious *a priori*. The situation is even less trivial if a planar array is made of semiconducting NTs. For a single semiconducting NT the charge separation happens for a field exceeding the critical value $F_{th} = E_g/2eh$. As F exceeds F_{th}, the charges occupy progressively larger portion of the NT; positive and negative charges are separated by a neutral strip[22] of a length E_g/eF. It is not obvious how, upon increasing F above F_{th}, the field-induced charge separation occurs in a planar array of semiconducting NTs. In particular, how the length of the neutral strip depends on the parameters of the array, namely, the length and density of constituting NTs.

The questions formulated above are addressed in the present paper. In Sect. II we extend the approach developed in Ref. 20 to the planar array of NTs. In Sect. III we demonstrate that for the planar array the Thomas-

Fermi equation can be solved *exactly* and find a simple analytical expression for the charge distribution along the NT for arbitrary external field. In particular, we find a universal relation between the length, $2h_0$, of the neutral strip and the applied field, F, and discuss qualitatively the limiting cases; Sect. IV. In Sect. V the exact form of the charge distribution is utilized to calculate analytically various characteristics of the array, such as (i) electric field inside the neutral strip, (ii) electric field outside the array, (iii) enhancement of the electric field near the tips of NTs, and ($iiii$) polarizability of NTs in the array. Concluding remarks are presented in Sect. VI.

II. THOMAS-FERMI EQUATION FOR THE PLANAR ARRAY

Derivation of the Thomas-Fermi for the planar array is completely analogous to that for vertical array[20] (see also Ref. 23) and goes as follows. The charge separation in a given NT of the array occurs due to the external field and the field, created by induced charges on all NTs. This separation proceeds until the local chemical potential assumes a constant value along each NT of the array. This local chemical potential of m-th NT, $\mu_m(z)$, is related to the local charge density via the NT electronic spectrum[20,22] as follows: $\mu_m(z) = sign(z)(E_g^2/4 + [\rho_m(z)/g]^2)^{1/2}$. Then the condition of the constant chemical potential can be presented in the form of generalized Thomas-Fermi equation, which for a given NT, m, in the array reads

$$
eFz - \int_{-h}^{h} dz' \sum_n \rho_n(z') \phi(z, z'; R_m - R_n),
$$
$$
= \text{sign}(z) \sqrt{\frac{E_g^2}{4} + \left[\frac{\rho_m(z)}{g}\right]^2}, \qquad (1)
$$

where $|R_n - R_m|$ is the distance between the centers of the NTs n and m. In Eq. (1) the dimensionless interaction parameter g is related to the electron velocity, v_0, in the NT as[20,22] $g = (2Ne^2/\pi\epsilon^*\hbar v_0)$, where N is the number of conducting channels, which assumes the values 2 or 4 depending on the spin and band degeneracy. This degeneracy is governed by the NT chirality. The potential, $\phi(z, z')$, in Eq. (1) is given by

$$
\phi(z, z'; R) = \frac{e}{\epsilon^* \sqrt{(z - z')^2 + R^2}}, \qquad (2)
$$

where $\epsilon^* = (\epsilon + 1)/2$ is the average dielectric constant between the substrate and the air. For a regular array we set all $\rho_n(z)$ equal to $\rho(z)$ and introduce the NT density, $\mathcal{N}_0$, as $\mathcal{N}_0 = 1/d$. As the next step, we take the continuous limit of Eq. (1). In doing so, we first isolate the NT with $n = 0$ and rewrite Eq. (1) in the form

$$
eFz = \text{sign}(z) \sqrt{\frac{E_g^2}{4} + \left[\frac{\rho(z)}{g}\right]^2} + 2\mathcal{L}_d \rho(z)
$$
$$
+ \frac{\mathcal{N}_0}{\epsilon^*} \int_0^h dz' \rho(z') \mathcal{S}(z, z'), \qquad (3)
$$

where $R_n = nd$, and the kernel, $\mathcal{S}(z, z')$, is defined as

$$
\mathcal{S}(z, z') = \sum_{n \neq 0} \left[\frac{1}{\sqrt{(z - z')^2 + R_n^2}} - \frac{1}{\sqrt{(z + z')^2 + R_n^2}} \right].
$$
$$(4)$$

Here we have used the fact that $\rho(z) = -\rho(-z)$. The term $2\mathcal{L}_d \rho(z)$ in the rhs of Eq. (3) comes from the term with $n = 0$ in the sum (1) and describes the "self-action" of a given NT. For an isolated NT[22] this term has the form $2\ln(h/r)\rho(z)$, where r is the NT radius. In the presence of neighboring NTs, the self-action is limited by the distance $\sim d$, so that $\mathcal{L}_d$ is equal to $\ln(d/r)$ analogously to the vertical array[20]. Now taking the continuous limit in Eq. (3) reduces to replacement the sum over n in the kernel Eq. (4) by the integral, leading to the following integral equation

$$
eFz = \text{sign}(z) \sqrt{\frac{E_g^2}{4} + \left[\frac{\rho(z)}{g}\right]^2}
$$
$$
+ 2\mathcal{L}_d \rho(z) + \frac{2\mathcal{N}_0}{\epsilon^*} \int_{-h}^{h} dz' \rho(z') \ln(|z - z'|). \quad (5)
$$

Rigorous justification of the continuous description is given in Appendix, where we show that the effect of discreteness of NTs in the array amounts to a small $\sim d/h$ correction to $\rho(z)$.

III. SOLUTION OF THE INTEGRAL EQUATION

A. Metallic NTs

In the case of metallic NTs we set $E_g = 0$ in Eq. (5). We will also neglect the self-action term, $2\mathcal{L}_d$, in the rhs; the validity of this step will be verified in the end of this Subsection. Then, for positive z, Eq. (5) takes the form

$$
eFz = \frac{2\mathcal{N}_0}{\epsilon^*} \int_0^h dz' \rho(z') \ln \left| \frac{z + z'}{z - z'} \right|. \qquad (6)
$$

Note that Eq. (6) does not contain any small parameter. Indeed, upon introducing dimensionless charge density and coordinate as

$$
\tilde{\rho} = \frac{\mathcal{N}_0}{e\epsilon^* F} \rho, \qquad \tilde{z} = \frac{z}{h}, \qquad (7)
$$

Eq. (7) assumes the following form

$$\tilde{z} = \int_0^1 d\tilde{z}' \, \tilde{\rho}(\tilde{z}') \, \ln \left| \frac{\tilde{z} + \tilde{z}'}{\tilde{z} - \tilde{z}'} \right|. \qquad (8)$$

In Eq. (8) the relevant values of $\tilde{\rho}$, z', and $\tilde{z}$ are all of the order of unity. It turns out, however, that, despite the absence of a small parameter, Eq. (8) can be solved analytically in the closed form. The solution reads

$$\tilde{\rho}(\tilde{z}') = \frac{\tilde{z}'}{\pi \sqrt{1 - (\tilde{z}')^2}}. \qquad (9)$$

In order to check that Eq. (9) is indeed the solution of the integral equation (8), we substitute (9) into the rhs of Eq. (8) and perform integration by parts as follows

$$\int_0^1 d\tilde{z}' \frac{\tilde{z}'}{\sqrt{1 - (\tilde{z}')^2}} \ln \left| \frac{\tilde{z} + \tilde{z}'}{\tilde{z} - \tilde{z}'} \right| \qquad (10)$$

$$= -2\tilde{z} \int_0^1 d\tilde{z}' \frac{\sqrt{1 - (\tilde{z}')^2}}{(\tilde{z}')^2 - \tilde{z}^2} = -2\tilde{z} \int_0^{\pi/2} d\varphi \frac{(\cos \varphi)^2}{(\sin \varphi)^2 - \tilde{z}^2},$$

where the integration in the rhs implies taking the principal value. The last identity in Eq. (10) emerges upon substitution $\tilde{z} = \sin \varphi$. Our key observation is that the integral in rhs is equal $-\pi/2$ for *all* $|\tilde{z}| < 1$, so that $\tilde{\rho}(\tilde{z})$ in the form (9) is indeed the solution of Eq. (8). Returning to dimensional variables, we present the final result for the charge density distribution in the form

$$\rho(z) = \frac{e\epsilon^* F z}{\pi \mathcal{N}_0 \sqrt{h^2 - z^2}}. \qquad (11)$$

Recall now, that this result was obtained neglecting the self-action. To verify the validity of this assumption, we estimate the ratio, $2\mathcal{L}_d \rho(z)/e\epsilon^* F z$, of the self-action term in Eq. (5) to the lhs. As follows from Eq. (11), this ratio is $\sim \mathcal{L}_d/\mathcal{N}_0 h$. Thus, the self-action can be neglected, if $\mathcal{N}_0 > \mathcal{L}_d/h$, i.e., when the array is sufficiently dense. Although the self-action term is relatively small, it overweighs the integral term near the tips, where the solution Eq. (11) diverges. This suggests that the divergence in (11) must be cut off at $(h - z) \sim h \left(\mathcal{L}_d/h\mathcal{N}_0 \right)^2$, where the the first term in the rhs of Eq. (5) becomes comparable to the lhs. At the cutoff, the ratio $(h - z)/h$ is $\sim \left(\mathcal{L}_d/h\mathcal{N}_0 \right)^2 \ll 1$, indicating that, in a dense array, the solution Eq. (11) applies up to the close vicinity of the tip.

B. Semiconducting NTs

1. Reduction of the Thomas-Fermi equation to the Hilbert form

Upon neglecting self-action, and in the limit of large g, the Thomas-Fermi equation for the charge distribution takes the form

$$eFz - \text{sign}(z) \frac{E_g}{2} = \frac{2\mathcal{N}_0}{\epsilon^*} \int_{-h}^h dz' \rho(z') \ln(|z - z'|). \quad (12)$$

As was explained qualitatively in the Introduction [see also Ref. (22)], in contrast to the metallic case, the solution of Eq. (12) is singular. This is because the positive and negative charges near the tips, induced by the external field, are separated by the neutral strip, caused by a finite bandgap, E_g, with boundaries at $z = \pm h_0$. Within this strip we have $\rho(z) = 0$. As the external field increases, the strip narrows. Solving Eq. (12) implies finding both the form of $\rho(z)$ outside the interval $[-h_0, h_0]$ and the dependence of h_0 on the external field.

Formally, with finite E_g, the integral equation contains one dimensionless parameter, E_g/eFh. In this subsection we demonstrate that the exact solution of Eq. (12) can be obtained for *arbitrary* value of this parameter. As a first step it is convenient to differentiate both sides of Eq. (12) with respect to z. This yields the following Hilbert-type integral equation

$$\frac{e\epsilon^* F}{2\mathcal{N}_0} = \int_{-h}^{-h_0} dz' \frac{\rho(z')}{z - z'} + \int_{h_0}^h dz' \frac{\rho(z')}{z - z'}. \qquad (13)$$

Our key observation is that the 2D geometry of the array allows one to employ the technique of conformal mapping in order to solve Eq. (13). The choice of the appropriate conformal transformation is described below.

2. Conformal Mapping

The conformal mapping method can be applied for large g, when each of the regions $-h < z < -h_0$ and $h_0 < z < h$ are *equipotential*. Then a general solution of the 2D Poisson equation with boundary conditions of equipotentiality on flat metal surfaces can be obtained from mapping of the boundaries of these surfaces on the real axis in the complex plane. What makes the case of semiconducting array nontrivial, is that the boundaries of equipotential regions have a doubly-connected geometry.

To gain an insight as to what is the appropriate form of the transformation for the geometry under study, it is instructive to start with an auxiliary problem of two *isolated* metallic plates in external field, occupying the intervals $[-h, -h_0]$ and $[h_0, h]$. Two metallic plates correspond to the two cuts on the complex plane, as shown in Fig. 2. The general solution of Eq. (13) for this geometry can be found in the textbooks[24,25,26,27]. It can be expressed through the integrals along the closed contours L_- and L_+, encompassing the cuts in the clockwise
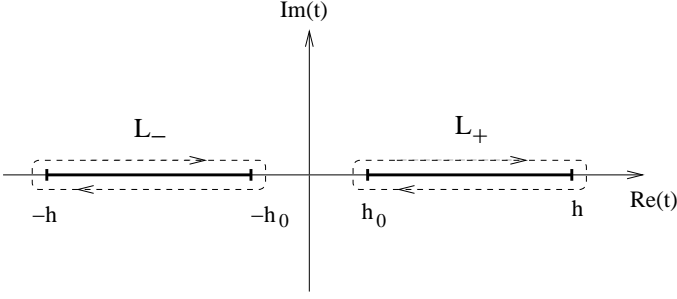
FIG. 2: Contours of integration in Eq. (14), L_- and L_+, encompassing the cuts in the clockwise direction.

direction, in the following way

$$\rho(z) = \frac{A}{\sqrt{(z^2 - h_0^2)(h^2 - z^2)}}$$
$$\times \left\{ \oint_{L_- \cup L_+} dt \, \frac{\sqrt{h^2 - t^2} \, \sqrt{t^2 - h_0^2}}{z - t} \right\}. \quad (14)$$

3. Solution for the charge density distribution

Although Eq. (14) satisfies Eq. (13), it cannot be applied to the planar array of semiconducting NTs. The reason lies in the fundamental difference between the isolated metallic plates and array of semiconducting NTs. In the former case *each* plate respects electroneutrality, i.e., $\int_{-h}^{-h_0} dz \rho(z) = 0$, $\int_{h_0}^{h} dz \rho(z) = 0$, while the array is neutral only *as a whole.* Still Eq. (14) can be modified to account for this difference. The modification amounts to adding a constant to the integral in Eq. (14) after which acquires the following form

$$\rho(z) = \frac{1}{\sqrt{(z^2 - h_0^2)(h^2 - z^2)}}$$
$$\times \text{sign}(z) \left\{ 2A \int_{h_0}^{h} dt \, \frac{t\sqrt{h^2 - t^2} \, \sqrt{t^2 - h_0^2}}{t^2 - z^2} + C \right\}. \quad (15)$$

It can be checked by a direct substitution that Eq. (15) is the solution of Eq. (13) for arbitrary C. On the other hand, with nonzero C, the net charge in each of the intervals $[-h, -h_0]$ and $[h_0, h]$ is finite. On the physical grounds, the value of the constant C should be now determined from the condition $\rho(h_0) = 0$, which fixes the ratio of the constants C and A at the value $C/A = -(\pi/2)(h^2 - h_0^2)$. The meaning of this condition is that the charge density vanishes at the boundaries of the neutral strip. It turns out that the result Eq. (15) can be greatly simplified. Namely, the integral can be evaluated *analytically* leading to the following simple expression for the induced charge density

$$\rho(z) = \text{sign}(z) \, \frac{e\epsilon^* F}{\pi \mathcal{N}_0} \sqrt{\frac{z^2 - h_0^2}{h^2 - z^2}}. \quad (16)$$

The relation between h_0 and E_g can be now established by substitution of the solution Eq. (15) with unknown constants A and h_0 into Eq. (13) and equating linear in z and constant terms to eFz and $E_g/2$, respectively. This yields $A = -\epsilon^* F/\pi^2 \mathcal{N}_0$ and the following transcendental equation for h_0

$$\frac{E_g}{2eFh} = \text{E}\left[\frac{h_0^2}{h^2}\right] - \left(1 - \frac{h_0^2}{h^2}\right) \text{K}\left[\frac{h_0^2}{h^2}\right], \quad (17)$$

where $\text{K}(x)$ and $\text{E}(x)$ are the elliptic integrals of the first and the second kind, respectively. In conclusion of this
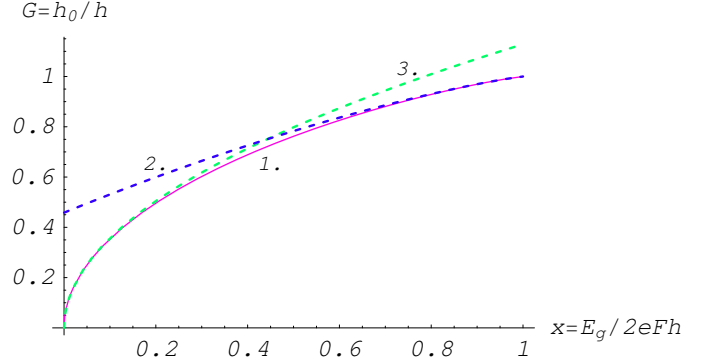

FIG. 3: (Color online) Curve 1: Dimensionless length of a neutral strip $G(x) = h_0/h$ is plotted versus dimensionless ratio $x = F_{th}/F$ from Eq. (17); Curves 2 and 3 are the asymtotes plotted from Eq. (19).

Section, we note that conformal mapping was previously employed to find the positions of boundaries of the two-dimensional electron gas in a smooth external potential[28] as well as to find the positions of edges of incompressible strips in the quantum Hall sample[29].

IV. DISCUSSION

Eq. (17) defines a universal dependence of the length, $2h_0$, of the neutral strip on the applied field, F. This dependence can be parameterized as

$$h_0 = h \, G\left(\frac{F_{th}}{F}\right), \quad (18)$$

where $F_{th} = E_g/2eh$ is the threshold value of F that causes the charge separation in the array. The dimensionless function, $G(x)$ is shown in Fig. 2. It has the following asymptotes

$$G(x) = \frac{2\sqrt{x}}{\sqrt{\pi}}, \qquad x \ll 1;$$
$$G(x) = 1 + \frac{2(1-x)}{\ln(1-x)}, \quad (1-x) \ll 1. \quad (19)$$

As seen from Fig. 2, the above asymptotes approximate $G(x)$ very closely. The dependence $G(x)$ should be contrasted to the corresponding dependence for an isolated NT, where it has the form[22] $G_0(x) = x$. We note, that $G(x) > G_0(x)$ for all x. In other words, the neutral strip for NT array is *wider* than that for a single NT. The difference is especially pronounced for strong fields, corresponding to $x \ll 1$, where we have $G(x)/G_0(x) \sim x^{-1/2}$. The origin of such a difference lies in the fact that the array screens the external field much more efficiently than a single NT. As a result, for strong fields, when $h_0 \ll h$, the field inside the strip is $\sim (h_0/h)$ times smaller than F. Then the condition that the potential drop within the neutral strip is equal to E_g can be presented as $eh_0(h_0F/h) \sim E_g$. This condition yields $h_0 \sim (E_g h/eF)^{1/2}$, which is in agreement with the small-x asymptote $G(x) \sim x^{1/2}$ of Eq. (19).

For an individual NT, the induced charge density changes linearly near the edges of the neutral strip[22]. By contrast, for a 2D array, $\rho(z)$ described by Eq. (16) exhibits a singular behavior, $\rho(z) \propto \pm\sqrt{z \pm h_0}$, near the boundaries of the neutral strip.

The principal assumption that allowed us to find the charge distribution in semiconducting NT analytically is that in Eq. (12) we had replaced $\sqrt{(E_g/2)^2 + (\rho/g)^2}$ in Eq. (5) by $E_g/2$. Using the result Eq. (16), we can now check the validity of this assumption. It is easy to see that the replacement is justified when the external field is not too strong, so that the dimensionless ratio $x = F_{th}/F$ in Eq. (19) must exceed the value $(g\mathcal{N}_0 h)^{-1} \ll 1$.

V. IMPLICATIONS

Exact results Eqs. (11), (16) for the charge distribution in metallic and semiconducting arrays, obtained above, enable us to calculate analytically various observable characteristics of the array. In this Section we will focus on the following characteristics: electric field distribution inside and outside of the array, and collective polarizability of the array. Concerning the electric field distribution, the questions most interesting for applications are the distribution of electric field within the neutral strips and behavior of electric field near the NT tips. The fist question is important for electrooptical measurements, while the second question is crucial for the field emission. In addition, it is instructive to study quantitatively how the charges, induced in the NTs by external field, alter this field in the regions above and below the array. In particular, the interesting question is how the spatial decay of the electric field component normal to the array depends on the position, z, along the NTs. These questions are addressed in subsections that follow.

A. Electric field inside the neutral strip

Electrostatic potential inside the neutral strip is given by superposition of the external potential, eFz, and the induced potential

$$\phi^{ind}(z) = \frac{2\mathcal{N}_0}{e\epsilon^*} \int_{h_0}^{h} dz' \rho(z') \ln\left|\frac{z+z'}{z-z'}\right|, \qquad (20)$$

where $z < h_0$. Upon substituting the exact form of the charge density, Eq. (16), in to Eq. (20) the integration can be performed analytically. We will present the result for the tangential component of the net electric field which is the sum of the external, F, and induced, $F_z^{ind} = \partial\phi^{ind}(z)/\partial z$, fields inside the neutral strip,

$$F_z^{st} = F_z^{ind} + F = F\sqrt{\frac{[h_0(F)]^2 - z^2}{h^2 - z^2}}, \qquad (21)$$

where the dependence $h_0(F)$ is defined by Eq. (17) and plotted in Fig. 3. In the limit of weak external field, close to the threshold value, F_{th}, Eq. (21) yields a natural result that $F_z^{st} \approx F$. This is because the induced charge occupies only a small portion, $(h - h_0) \ll h_0$, of the NTs. In the opposite limit of the strong external field, $F \gg F_{th}$, the field, F_z^{st}, at the center of the NTs is equal to $Fh_0[F]/h \ll F$, i.e., it is strongly suppressed, and falls off towards the ends of the strip. Note, that in our qualitative derivation of the width of the neutral strip we have used the estimate $F_z^{st} \sim Fh_0/h$ for the field inside the strip. Therefore, Eq. (21) justifies this estimate. The reason why we focused on the tangential component, F_z^{st}, is its possible relevance for the experiment[30] on electroabsorption of light. It might seem that, with photon energy $\sim$ 1eV much bigger than eFh, the large-scale nanotube geometry is not important. This, however, is not the case. The reason is that the dipole moment of the many-body optical transition is directed *along* the tube[31,32,33,34,35]. In analysis of the data in Ref. 30 it was assumed that in the change, $[\alpha(\omega, F_z) - \alpha(\omega, 0)]$, of the absorption coefficient, F_z is the *external* field. Meanwhile, the optical transition is modified by the *acting* field, F_z^{st}. Then Eq. (21) suggests that the acting field can be much smaller than the external field and, moreover, behaves as $F_z^{st} \propto F^{1/2}$ due to the collective screening.

B. Electric field outside the array

Consider a point with coordinate, z, located at a distance, H, above the array. Similarly to Eq. (21), the parallel and perpendicular components of the acting field

can be evaluated from

$$F_z(z, H) = F - \frac{\partial}{\partial z} \int_{-h}^{h} dz' \int_{-\infty}^{\infty} dx \frac{\mathcal{N}_0 \rho(z')}{\left[(z'-z)^2 + x^2 + H^2\right]^{1/2}},$$

$$F_\perp(z, H) = -\frac{\partial}{\partial H} \int_{-h}^{h} dz' \int_{-\infty}^{\infty} dx \frac{\mathcal{N}_0 \rho(z')}{\left[(z'-z)^2 + x^2 + H^2\right]^{1/2}}.$$

$$(22)$$

We will restrict ourselves to metallic NTs. In this case the integration in Eq. (22) can be performed analytically, yielding

$$F_z = \frac{F}{\sqrt{2\Lambda}} \sqrt{(z^2 + H^2)\sqrt{\Lambda} + \Lambda - h^2(h^2 + H^2 - z^2)},$$

$$F_\perp = \frac{\sqrt{2}F}{\sqrt{\Lambda}} \sqrt{(z^2 + H^2)\sqrt{\Lambda} - \Lambda + h^2(h^2 + H^2 - z^2)},$$

$$(23)$$

where we had introduced an auxiliary function $\Lambda(z, H)$ defined as follows

$$\Lambda(z, H) = (H^2 + z^2 - h^2)^2 + 4h^2 H^2. \qquad (24)$$

Eq. (23) allows one to trace how the tangent component, F_z, grows from zero to F with increasing H, while the normal component falls off from $2\pi \mathcal{N}_0 \rho(z)$ to zero with increasing H. The characteristic scale of change for both components is $H \sim h$. This behavior is illustrated in Fig. 4.
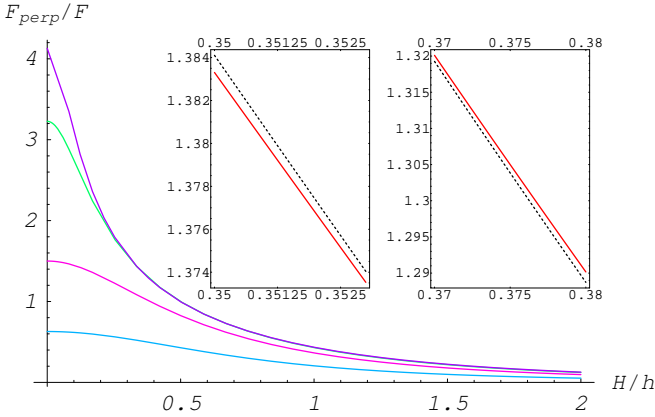

FIG. 4: (Color online) Dimensionless normal component, $F_\perp/F$, of the net electric field is plotted from Eq. (23) vs. dimensionless distance, H/h, from the array for various values of coordinate, z, along the array. The plots are presented from bottom up: $z/h = 0.3$; 0.6; 0.85; 0.9. Two insets illustrate that the curves $F_\perp(H)$ for $z/h = 0.8$ and $z/h = 0.9$ intersect each other. The actual point of intersection (not showed) is at $H/h \approx 0.3677$.

We see that, as could be expected, $F_\perp$ falls off monotonically with increasing the distance, H, from the array. Less trivial is that the curves for $z/h = 0.85$
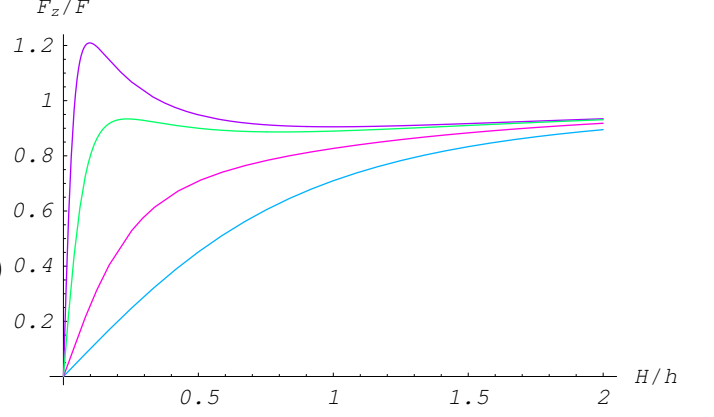

FIG. 5: (Color online) Dimensionless tangent component, F_z/F, of the net electric field is plotted from Eq. (23) vs. dimensionless distance, H/h, from the array for various values of coordinate, z, along the array. The plots are presented from bottom up: $z/h = 0.1$; 0.7; 0.9; 0.95.

and $z/h = 0.9$ intersect at $H/h \approx 0.3677$ (see inset in Fig. 5). This implies that the derivative $\partial F_\perp/\partial z$ is zero at this point. On the other hand the relation $\partial F_\perp/\partial z = \partial F_z/\partial H$ suggests that $F_z(H)$ must have a maximum at $H/h \approx 0.3$. As seen from Fig. 5, this is indeed the case. It is also seen from Fig. 4 that, for z/h approaching 1, the field $F_\perp$ grows in the vicinity of the plane of the array $H \to 0$. This is the manifestation of the enhancement of electric field near the tip. We address this issue in more detail in the next subsection.

C. Field enhancement near the tips

Consider a point, z_0, on the axis of one of the NTs outside the array, $z_0 > h$. The field in this point has only z-component given by

$$F_z^{ind} = \frac{\mathcal{N}_0}{e\epsilon^*} \int_0^h dz \rho(z) \left(\frac{1}{z_0 + z} - \frac{1}{z_0 - z}\right). \qquad (25)$$

With metallic charge density distribution Eq. (11) the integration in Eq. (25) can be performed analytically. We will present the result for the field enhancement factor, $\beta = F_z^{ind}/F$, which is the conventional characteristics of the field near the tip

$$\beta = \frac{h^2}{\sqrt{z_0^2 - h^2}\,(z_0 + \sqrt{z_0^2 - h^2})}. \qquad (26)$$

We can now compare the dependence $\beta(z_0)$ for the planar array and for an isolated NT. For the isolated NT we have[22] $\beta(z_0) \propto h/(z_0 - h)$ (in the present notations). By contrast, Eq. (26) yields a slower decay, $\beta(z_0) \sim h^{1/2}/(z_0 - h)^{1/2}$. On the other hand, the magnitude of the enhancement factor is much weaker for the planar array than for the isolated NT. Obviously, this reduction is due to the collective screening.

D. Induced dipole moment

The dipole moment, P, of a given NT within the array is defined as

$$P(F) = 2 \int_{h_0}^{h} dz \ z\rho(z). \tag{27}$$

Analytical evaluation of the integral in Eq. (27), with the charge density (16), yields the following expression for the dipole moment

$$P(F) = \frac{e\epsilon^* F}{4\mathcal{N}_0} \big(h^2 - \{h_0(F)\}^2 \big). \tag{28}$$

It is instructive to consider the limiting cases of weak and strong fields. Using the low-field and strong-field asymptotes of $h_0(F)$ given by Eq. (19), we obtain

$$P(F) = \left(\frac{e\epsilon^* F_{th} h^2}{\mathcal{N}_0} \right) \frac{1 - \frac{F_{th}}{F}}{\left| \ln\left[1 - \frac{F_{th}}{F} \right] \right|}, \quad (F - F_{th}) \ll F_{th},$$

$$P(F) = \frac{e\epsilon^* F h^2}{4\mathcal{N}_0} \left(1 - \frac{4F_{th}}{\pi F} \right), \qquad F \gg F_{th}. \tag{29}$$

Note that in the limit of low fields, $(F - F_{th}) \ll F_{th}$, the behavior of $P(F)$ is singular, unlike the individual NT, where one has[22] $P(F) \propto [1 - F/F_{th}]^2$. This singularity is the manifestation of the singular behavior of the charge density, $\rho(z) \propto \sqrt{z - h_0}$, at the boundary of the neutral strip. By contrast, for the individual NT, this behavior is regular, namely $\rho(z) \propto (z - h_0)$.

In the strong-field limit, the contribution of the neutral strip to $P(F)$ constitutes a relatively small correction $\sim F_{th}/F$. Essentially, the polarizability $\chi = P(F)/F$ of a given NT is $\sim eh^2/\mathcal{N}_0$, as seen from Eq. (28). On the other hand, the value of χ for the individual NT can be estimated from the textbook problem[36] of polarization of an ellipsoid with large ratio of axes in electric field directed along the major axis. With logarithmic accuracy one has, $\chi \sim eh^3$. Thus, compared to the individual NT, the polarizability of a given NT within the array is suppressed by a large factor $\mathcal{N}_0 h$. This conclusion can be reformulated as follows. An element of the array of a width h contains $\mathcal{N}_0 h$ NTs. The integral polarizability of this element is $\sim (\mathcal{N}_0 h)(eh^2/\mathcal{N}_0) = eh^3$, i.e., it is of the same order as polarizability of the individual NT. Therefore, the magnitude of suppression of χ within the array, can be understood from the fact that, within the array, the constituting NTs "talk to each other" only if their separation is smaller than h.

VI. CONCLUDING REMARKS

Throughout the paper we assumed that the NTs in the planar array are parallel to each other. Note, that recently a different class of planar NT arrays in the form of a *random network*, residing on the polymeric substrate, and connecting the source and drain electrodes has been discussed and realized experimentally[37,38,39]. It was demonstrated that such a network can emulate the channel of the field-effect transistor. Since in our consideration of the planar array was carried in continuous limit, the results obtained are relevant to the random planar dense arrays.

Our main results are Eqs. (11), (16) describing the distribution of induced charge in metallic and semiconducting planar arrays, respectively. These results were obtained in the continuous limit, i.e., we replaced the array of individual NTs with a two-dimensional continuous layer of a zero width. Such a replacement is justified with high accuracy as long as the NT length, h, exceeds the separation, d, between the neighboring NTs. More quantitatively, as shown in Appendix, the relative correction to the induced charge distribution is $\sim d/h$. Similarly, the randomness in distances between the neighboring NTs is not important for the planar array. This should be contrasted to the *infinite* vertical array[20], where the distance between *neighboring* NTs governs the penetration depth of the external field. By contrast, the continuous description adopted in the present paper applies with high accuracy, since, in the planar array, the induced charge extends over the entire length, $2h$, of the NTs. This length the is much bigger than $\mathcal{N}_0^{-1}$. The discreteness of the array manifests itself only in the close vicinity of the tips, where it cuts off the singularity $\rho(z) \propto (h - z)^{-1/2}$ in the distribution of the induced charge.

It is instructive to trace how the results obtained in the present paper for the planar array evolve when one considers the vertical array of a *finite* thickness, W. Consider first the most interesting case of intermediate thickness, $d \ll W \ll h$. The modification of our result Eq. (11) to this case can be understood from the following reasoning. Each square with the side W contains $(W/d)^2$ NTs. This square can be viewed as a single "combined" NT. Then the charge density in this combined NT is given by Eq. (11) with $\mathcal{N}_0$ replaced by W^{-1}. To find the charge density *per a single* NT, this result should be divided by $(W/d)^2$. Thus we conclude, that modification of Eq. (11) to finite $W < h$ amounts to the replacement of $\mathcal{N}_0^{-1}$ by d^2/W, so that the induced charge density falls off as $1/W$ with increasing the width. However, the applicability of Eq. (11) to the finite-width array is limited by the size of a "combined" NT, i.e., $(h - z)$ must exceed W. As W exceeds the NT length, this condition cannot be met, and the charge distribution changes dramatically from the power-law behavior to the exponential screening[20].

Note that our basic integral equation, Eq. (5), expressing the fact that electrochemical potential is constant along each NT of the array allow the exact solution using the technique of conformal mapping only when the "self-action" [second term in the rhs of Eq. (5)] is neglected. This step is well justified for a dense array. In the electrostatics of inhomogeneous fractional quantum

Hall liquids[40,41] the charge distribution is described by the equations similar to Eq. (5), i.e., with logarithmic kernel, but with self-action playing an important role. Then these equations can be solved only numerically.

Acknowledgments

VII. APPENDIX

Below we present a rigorous derivation of Eq. (5) for a periodic array of NTs. We start from the identity

$$\frac{1}{\sqrt{x^2 + b^2}} = \frac{1}{\pi} \int_{-\infty}^{\infty} dq \, K_0\Big(|x| \, q\Big) \exp(iqb), \tag{30}$$

where $K_0(x)$ is the modified Bessel function of the second kind. To use this identity in Eq. (3), we set $b \to R_n = nd$. Then the summation in the integrand in the rhs can be readily performed; it transforms the sum over n in Eq. (4) into the following sum of the δ-functions

$$\sum_n \exp(iqR_n) = \frac{2\pi}{d} \sum_p \delta\left(q - \frac{2\pi p}{d}\right), \tag{31}$$

where p assumes *all* integer values. As the next step we isolate the term with $p = 0$ in the kernel Eq. (4) from all other terms with nonzero p. Then we make use of the fact, that

$$K_0(x) = -\gamma + \ln 2 - \ln|x| + O(x^2), \qquad x \ll 1, \tag{32}$$

where γ is the Euler constant. Then, for the term with $p = 0$, we get

$$\frac{2}{d} \lim_{q \to 0} \big[K_0(|z - z'|q) - K_0(|z + z'|q) \big] = \frac{2}{d} \ln\left|\frac{z - z'}{z + z'}\right|. \tag{33}$$

Therefore, after performing the summation over n in Eq. (4) and using Eq. (33), the rhs of Eq. (3) will acquire the form

$$\int_0^h dz' \rho(z') \mathcal{S}(z, z'), \tag{34}$$

where the kernel $\mathcal{S}(z, z')$ is given by

$$\mathcal{S}(z, z') = \frac{2}{d} \ln\left|\frac{z - z'}{z + z'}\right| \tag{35}$$
$$+ \frac{2}{d} \sum_{p \neq 0} \left[K_0\Big(|z - z'| \frac{2\pi p}{d}\Big) - K_0\Big(|z + z'| \frac{2\pi p}{d}\Big) \right].$$

First term in (35) describes the continuous limit; it reproduces the second term in the rhs of Eq. (5) and comes from $p = 0$ in Eq. (31). The remaining sum over p gives rise to the "self-action" term in Eq. (5). The easiest way to see this is to replace the summation over p by integration dp, which would immediately yield

$$S_0(z, z') = \phi(z - z') - \phi(z + z') \tag{36}$$

for the second part of the kernel (35). Note that $S_0(z, z')$ is nothing but the kernel for a *single* NT[20,22]. However, the replacement of the $\sum_{p \neq 0}$ by $\int dp$ is justified only when a large number of terms contribute to the sum. This is the case only when the condition $|z - z'| \lesssim d$ is met. Then, upon substituting (36) into (31) and restricting integration over z' to $|z' - z| \lesssim d$, the self-action term in Eq. (5) is recovered. Concerning the second part of the kernel (35) at $|z' - z| > d$, it is dominated by the terms with $p = \pm 1$, which behave as $\left(d/|z - z'|\right)^{1/2} \exp\left\{-2\pi|z - z'|/d\right\}$. Contribution coming from this part to the integral Eq. (34) is $\sim \rho(z)$, which is parametrically smaller than the self-action term $2\mathcal{L}_d \rho(z)$.

[1] M. Terrones, N. Grobert, J. Olivares, J. P. Zhang, H. Terrones, K. Kordatos, W. K. Hsu, J. P. Hare, P. D. Townsend, K. Prassides, A. K. Cheetham, H. W. Kroto, and D. R. M. Walton, Nature (London) **388**, 52 (1997).

[2] Z. F. Ren, Z. P. Huang, J. W. Xu, J. H. Wang, P. Bush, M. P. Siegal, and P. N. Provencio, Science **282**, 1105 (1998).

[3] Q. H. Wang, A. A. Setlur, J. M. Lauerhaas, J. Y. Dai, E. W. Seelig, and R. P. H. Chang, Appl. Phys. Lett. **72**, 2912 (1998).

[4] S. Fan, M. G. Chapline, N. R. Franklin, T. W. Tombler, A. M. Cassell, and H. Dai, Science **283**, 512 (1999).

[5] O. Gröning, O. M. Küttel, Ch. Emmenegger, P. Gröning, and L. Schlapbach, J. Vac. Sci. Technol. B **18**, 665 (2000).

[6] L. Nilsson, O. Groening, C. Emmenegger, O. Kuettel, E. Schaller, L. Schlapbach, H. Kind, J.-M. Bonard, and K. Kern, Appl. Phys. Lett. **76**, 2071 (2000).

[7] J.-M. Bonard, K. A. Dean, B. F. Coll, and C. Klinke, Phys. Rev. Lett. **89**, 197602 (2002).

[8] F. Picaud, R. Langlet, M. Arab, M. Devel, C. Girardet, S. Natarajan, S. Chopra, and A. M. Rao, J. Appl. Phys. **97**, 114316 (2005).

[9] V. I. Merkulov, D. H. Lowndes, and L. R. Baylor, J. Appl. Phys. **89**, 1933 (2001).

[10] M. Chhowalla, C. Ducati, N. L. Rupesinghe, K. B. K. Teo, and G. A. J. Amaratunga, Appl. Phys. Lett. **79**, 2079 (2001).

[11] J. S. Suh, K. S. Jeong, J. S. Lee, and I. Han, Appl. Phys. Lett. **80**, 2392 (2002).

[12] H. J. Lee, S. I. Moon, J. K. Kim, Y. D. Lee, S. Nahm, J. E. Yoo, J. H. Han, Y. H. Lee, S. W. Hwang, and B. K. Ju, J. Appl. Phys. **98**, 016107 (2005).

[13] A. Ural, Y. Li, and H. Dai , Appl. Phys. Lett. **81**, 3464 (2002).

[14] A. Nojeh, A. Ural, R. F. Pease, and H. Dai, J. Vac. Sci. Technol. B **22**, 3421 (2004).

[15] Z. J. Zhang, B. Q. Wei, G. Ramanath, and P. M. Ajayan, Appl. Phys. Lett. **77**, 3764 (2000).

[16] Z. J. Zhang, P. M. Ajayan, G. Ramanath, J. Vacik and Y. H. Xu, Appl. Phys. Lett. **78**, 3794 (2001).

[17] A. Cao, B. Wei, Y. Jung, R. Vajtai, P. M. Ajayan, and G. Ramanath, Appl. Phys. Lett. **81**, 1297 (2002).

[18] V. V. Tsukruk, H. Ko, and S. Peleshanko, Phys. Rev. Lett. **92**, 065502 (2004).

[19] L. Nilsson, O. Groening, C. Emmenegger, O. Kuettel, E. Schaller, L. Schlapbach, H. Kind, J.-M. Bonard, and K. Kern, Appl. Phys. Lett. **76**, 2071 (2000).

[20] T. A. Sedrakyan, E. G. Mishchenko, and M. E. Raikh, Phys. Rev. B **73**, 245325 (2006).

[21] M. Wang, Z. H. Li, X. F. Shang, X. Q. Wang, and Y. B. Xu, J. Appl. Phys. **98**, 014315 (2005).

[22] E. G. Mishchenko and M. E. Raikh, Phys. Rev. B **74**, 155410 (2006).

[23] M. P. Anantram and F. Léonard, Rep. Prog. Phys. **69**, 507 (2006).

[24] N. I. Muskhelishvili, *Singular Integral Equations; Boundary Problems of Function Theory and Their Application to Mathematical Physics*, Groningen, P. Noordhoff, 1953.

[25] Z. Nehari, *Conformal mapping* , New York, McGraw-Hill, 1952.

[26] T. A. Driscoll and L. N. Trefethen, *Schwarz-Christoffel Mapping*, Cambridge University Press, 2002.

[27] V. I. Ivanov and M. K. Trubetskov, *Handbook of Conformal Mapping with Computer-Aided Visualization*, CRC Press, 1995.

[28] L. I. Glazman and I. A. Larkin, Semicond. Sci. Technol. **6**, 32 (1991).

[29] D. B. Chklovskii, B. I. Shklovskii, and L. I. Glazman, Phys. Rev. B **46**, 4026 (1992).

[30] J. W. Kennedy, Z. V. Vardeny, S. Collins, R. H. Baughman, H. Zhao, S. Mazumdar, preprint cond-mat/0505071.

[31] C. L. Kane and E. J. Mele, Phys. Rev. Lett. **90**, 207401 (2003); **93**, 197402 (2004).

[32] C. D. Spataru, S. Ismail-Beigi, L. X. Benedict, and S. G. Louie, Phys. Rev. Lett. **92**, 077402 (2004);

[33] V. Perebeinos, J. Tersoff, and P. Avouris, Phys. Rev. Lett. **92**, 257402 (2004).

[34] W.-Z. Liang, G.-H. Chen, Z. Li, and Z.-K. Tang, Appl. Phys. Lett. **80**, 3415 (2002).

[35] H. Zhao and S. Mazumdar, Phys. Rev. Lett. **93**, 157402 (2004).

[36] L. D. Landau and E. M. Lifshitz, *Electrodynamics of Continuous Media* (Pergamon Press, Oxford, 1984).

[37] E. S. Snow, J. P. Novak, P. M. Campbell, and D. Park, Appl. Phys. Lett. **82**, 2145 (2003).

[38] E. S. Snow, P. M. Campbell, M. G. Ancona, and J. P. Novak, Appl. Phys. Lett. **86**, 033105 (2005).

[39] S. Kumar, N. Pimparkar, J. Y. Murthy, and M. A. Alam, Appl. Phys. Lett. **88**, 123505 (2006).

[40] I. Kogan, A. M. Perelomov, and G. W. Semenoff, Phys. Rev. B **45**, 12084 (1992).

[41] J. Shiraishi, Y. Avishai, and M. Kohmoto, Phys. Rev. B **57**, 13061 (1998).